Biomechanical Investigation of Head Kinematics and Skull Stiffness

Christina Nocon Seimetz

Thesis submitted to the faculty of the Virginia Polytechnic Institute and State University
in partial fulfillment of the requirements for the degree of

Master of Science
In
Biomedical Engineering

Stefan M. Duma
Andrew R. Kemper
Hampton C. Gabler
Warren N. Hardy
Per Gunnar Brolinson

May 31, 2011
Blacksburg VA

Keywords: biomechanics, head, skull stiffness, cranial motion, kinematics, trajectory

Biomechanical Investigation of Head Kinematics and Skull Stiffness

Christina Nocon Seimetz

ABSTRACT

This thesis presents two studies related to head injury. The study presented in Chapter 1 reviewed findings of cranial movement in animal and human specimens and evaluate the validity of cranial movement due to manual manipulation in humans through engineering analysis. The study had two parts. In Part I, the literature was reviewed to determine the cranial motion in animals and humans. Engineering analysis was done in Part II to determine the amount of force necessary to cause cranial motion in the studies from Part I using skull stiffness values from published studies.

Chapter 2 explored data collection methodologies used in frontal sled tests. Several data collection methodologies exist for collecting kinematic data, such as Vicon motion analysis, video analysis, and sensors. Head trajectories from motion data and accelerometer data were plotted up to maximum forward excursion of the head for eight frontal sled tests, four conducted at Virginia Tech and four at the University of Virginia. In addition, the percent difference between maximum forward excursion values from sensor and motion data were calculated. Finally, Chapter 3 discusses the literary contributions of each study and to which journals they will be submitted.

TABLE OF CONTENTS

LIST OF FIGURES

LIST OF TABLES

CHAPTER 1

AN INVESTIGATION OF CRANIAL MOTION THROUGH AN ENGINEERING ANALYSIS OF SKULL DEFORMATION

Objectives: There is ongoing debate over the existence of cranial motion, especially in its application of Cranial Osteopathy (CO). The purpose of this study was to review findings of cranial movement in animal and human specimens and evaluate the validity of cranial movement due to manual manipulation in humans through engineering analysis.
Methods: In Part I, the literature was reviewed to determine the cranial motion in animals and humans. Engineering analysis was done in Part II to determine the amount of force necessary to cause cranial motion in the studies from Part I using skull stiffness values from published studies.
Results: Skull deflection in animals ranged from 0µm to 910µm. Skull deflection in humans ranged from 0µm to 3.72µm. Engineering analysis resulted in a wide range of forces, between 0.44N and 111N (25lb), necessary to cause reported deflections in humans. Studies that have determined the forces applied during CO have measured forces ranging from 0.13N to 8.2N. However, the studies investigating the amount of pressure applied during CO took measurements from only one finger. Osteopathic physicians typically use more than one finger during manual manipulation. Therefore, the total amount of pressure applied to the skull during CO should be greater than the pressures reported in the palpation studies.
Conclusion: While the amount of cranial motion may vary by subject and the region of the head on which forces are applied, it is reasonable that small amounts of cranial motion may occur during CO. However, there is no existing evidence as to whether cranial motion contributes to the reduction in symptoms that results from CO. Patient improvement may be attributed to several different mechanisms such as: a placebo effect, relaxation of muscles due to massaging effects, decrease in pressure on the cranial nerves due to massaging effects. Therefore, further research should be conducted to investigate the effects of cranial motion in CO.

Keywords: cranium, osteopathy, rhythm, cranial movement, skull deflection, stiffness, biomechanics

Introduction

Awareness of head injuries and concussions in sports, such as baseball[1] and football[2-5], has increased over the past few years. Head injuries and concussions are also seen in the automotive industry[6] and the military[7]. Symptoms of these injuries can be treated with Cranial Osteopathy (CO), also referred to as Osteopathy in the Cranial Field (OCF). Several studies report that CO has successfully improved symptoms of neurological and medical problems in children[8,9,10] and adults[11,12] including but not limited to: infantile colic[9], infantile gastroesophageal reflux[10], vision impairment[11], and lasting effects of brain injury[12].

In 1899, Dr. William G. Sutherland began the development of CO[13]. This treatment approach includes manual manipulation of the cranial bones, membranes and fluids. In addition, CO is based on the existence of the Primary Respiratory Mechanism (PRM). The PRM includes

five physiological and functionally anatomical phenomena: inherent rhythmic motion of the brain and spinal cord; fluctuation of cerebral spinal fluid; mobility of intracranial and intraspinal membranes; articular mobility of the cranial bones; and involuntary mobility of the sacrum between the ilia. The PRM can be palpated anywhere on the body, which allows for treatment through CO to be applied to the entire body. The motion palpable through placement of hands on the cranium is termed Cranial Rhythmic Impulse (CRI). Cranial bone mobility has been described to occur mainly at the cranial sutures.

Several studies have been conducted to investigate the existence and palpation of CRI [14-16], as well as movement of the cranial bones. Studies investigating cranial rhythm have mixed findings on its existence and practitioners' abilities to recognize CRI during palpation[14-16]. Moran and Gibbons[14] conducted a study in which two Australian osteopathic physicians were asked to identify the CRI in eleven healthy subjects by simultaneous palpation at the head [*CRI*] and sacrum [*PRM*]. One osteopathic physician palpated the head while the other palpated the sacrum. Although both physicians were able to detect a rhythmic motion, the frequencies of the rhythms reported by each osteopathic physician did not agree. Wirth and Hayes[15] asked three therapists to palpate twelve subjects, both children and adults, with a history of physical trauma. During the assessment, the heart and respiratory rates of the subjects and therapists were measured. While the cranial rhythms reported by the physical therapists were not related to the heart and respiratory rates of either the therapist or the subject, there was a lack of agreement of the rhythmic patterns observed by each therapist. Michael and Retzlaff[16] measured heart rate, blood pressure, and parietal bone movement in anesthetized adult squirrel monkeys. They identified a rhythmic displacement of the parietal bone that was not linked to respiration or heart rate.

Similar to studies of CRI, there have been mixed findings of the existence of cranial mobility[17-21]. In addition, many medical professionals believe that motion across the cranial sutures is not possible, leading to an ongoing debate of the topic[13]. This study approached the debate from an engineering perspective. The purpose of this study was to review findings of cranial movement in animal and human specimens and evaluate the validity of cranial movement due to manual manipulation in humans through engineering analysis.

Methods

This study was conducted in two parts. Part I reviewed published studies of cranial motion. Part II investigated the validity of the cranial motion measurements from the published studies in Part I by determining if the forces required to cause cranial motion can be generated during CO.

Part I: Review of Cranial Motion

Published studies investigating cranial motion of animals and humans were briefly summarized. This motion was a result of induced stress, internal or external, on the skull. Internal stress was generated by increasing intracranial pressure. External stress was generated by exerting forces on the body manually or through means of an apparatus. Measured values of cranial motion were reported for each specimen.

Part II: Engineering Analysis

Published studies investigating the mechanical stiffness of the whole skull or regions of the skull were summarized, including a brief description of methods and the reported stiffness values. Skull stiffness values were then used to calculate the amount of external force required to induce cranial motion in human specimens.

Results

Six published studies investigating cranial motion are reviewed in Part I of the results. Three studies performed tests on animal specimens, and two studies performed tests on human specimens. The sixth study performed testing on both animals and humans. Part II reports human skull stiffness values from six studies and results of the engineering analysis on cranial motion.

Part I: Review of Cranial Motion

Animal Studies

Pitlyk et al.[17] used strain gauges to measure cranial movement due to changes in intracranial pressure in six dogs. Intracranial pressure was increased with a balloon inserted into the subarachnoid space of the brain and attached to the end of a catheter or by injections of saline into the spine. Stain gauges were attached to an apparatus that arched mediolaterally across the head to measure changes in skull diameter. Although quantitative data for cranial motion was not reported in the publication, the study concluded that cranial movement correlates to an increase in intracranial pressure (Table 1).

Oudhof et al.[18] used strain gauges to measure deflection between the sagittal and coronal sutures in six-week old and three-year old beagles. While no deflection was seen in the skulls of the adults beagles, movement of 5-10μm was observed in the beagle puppies (Table 1). Measurements of carbon dioxide (CO_2) content in the blood, aortic pressure, and an electrocardiogram (ECG) were also obtained during the study. It was found that the skull deflection patterns matched changes in aortic flow and ECG.

A study conducted by Downey et al.[19] in 2000 observed separation across the coronal suture in New Zealand white rabbits. Brackets were mounted to the skull on either side of the

suture and used to apply tension across the suture. All subjects were exposed to 5, 10, 15, and 20 grams of force. One subject experienced additional loads of 100 grams to 10,000 grams. Radiographs were taken of each subject's skull during exposure to load and used to determine the amount of separation at the coronal suture. Skull deflection resulting from most of the forces was not significant. However, the subject that experienced the additional loads between 100 grams and 10,000 grams showed separation of the coronal suture up to 0.31mm at 5,000 grams and 0.91mm at 10,000 grams (Table 1).

In 1992, movement across the sagittal suture of anesthetized cats was measured by Adams et al.[20] An apparatus that had two strain gages to measure cranial motion was placed across the sagittal suture (Table 1). Cranial motion was induced by various external an internal forces exerted on the skull (Table 2). External forces included manual compression of the sides of the skull, manually applied downward force on the sagittal suture, and a 2.2N compressive or tensile force applied by a spring on the parietal bones. Three different methods were used to exert internal forces on the skull which aimed to increase intracranial pressure: induced hypercapnia by inhaling excess CO_2; intravenous injection of norepinephrine; and injection of artificial cerebrospinal fluid (CSF).

Table 1. Cranial movement in various specimens

Author	Specimen	Skull deflection (μm)
Pitlyk et al.[17]	Dog	0
Oudhof et al.[18]	Beagle puppy	5-10
	Grown beagle	0
Downey et al.[19]	Rabbit	310-910
Adams et al.[20]	Cat	30-75

Table 2. Cranial movement in anesthetized cat		
Force type		**Skull deflection (µm)**
External	Manual compression of sides of head	65
	Manual downward force on sagittal suture	30
	Spring compression	40
	Spring tension	75
Internal	Induced hypercapnia	30
	Norepinephrine injection	50
	Artificial CSF	50

Human Studies

Pitlyk et al.[17] observed minute cranial motion of a dry cadaver skull and fresh cadaver skulls, with the skin and intracranial contents intact. Strain gauges attached to an apparatus that was placed across the medial-lateral diameter of the skull measured changes in diameter. Cranial movement resulted from force applied to the outside of the dry skull (direction of force not specified) and increased intracranial pressure in the cadaver. Intracranial pressure was increased by intraspinal injections of saline. Quantitative measurements of cranial motion were not reported (Table 3). However, qualitative data from the publication supported the existence of cranial motion. It was determined that there is a correlation between the amount of saline injected into the spine and the amount of cranial motion.

In 1981, Heifetz et al.[21] used an apparatus, instrumented with strain gages, placed across the medial-lateral diameter of the skull to measure changes in the diameter due to an increase in intracranial pressure in two comatosed patients. The total intracranial pressure was elevated to between 15mmHg to 20 mmHg using a different method in each patient. In Case 1, pressure was raised via bilateral jugular compression. In Case 2, the cranial ventricles were infused with 7-12cc of Ringer's lactate solution. The average skull movement detected was 3.72µm in Case 1 and 0.78µm in Case 2 (Table 3).

Table 3. Cranial movement in various specimens	
Author	**Skull deflection (μm)**
Pitlyk et al.[17]	No data reported
Heifetz et al.[21]	3.72
	0.78

Part II: Engineering Analysis

Skull Stiffness

Several studies have investigated the stiffness characteristics of the skull by region and as a whole. The publications reviewed in this study utilized different methodologies to quantify skull stiffness such as: mechanical impedance, impact tests, and drop tests.

Three studies[22-24] determined skull stiffness through mechanical impedance techniques. A force generator was attached directly to a cadaver skull to exert low-amplitude, sinusoidal forces of varying frequencies at the point of contact. The motion of the skull and forces exerted on the skull were recorded. The response of the skull varied with respect to frequency. Two frequencies of interest were those at antiresonance, where skull stiffness is the greatest, and resonance, where the skull stiffness is the lowest. The skull stiffness at antiresonance is most applicable to the current study because such conditions are comparable to manual manipulation.

Stalnaker et al.[22] used mechanical impedance techniques to quantify skull stiffness of a human cadaver head between frequencies of 30Hz and 5000Hz. Antiresonance was reported as 166Hz with a corresponding skull stiffness of 4553N/mm while resonance was reported at 820Hz (Table 4). No corresponding stiffness was reported for the resonance frequency.

A study conducted by Hodgson et al.[23] quantified the dynamic stiffness of the frontal, side parietal, top parietal, and occipital regions of the skull over a frequency range of 5Hz to 5000Hz. Antiresonance frequencies and the corresponding stiffness varied by region (Table 4).

Resonance frequencies also varied by region, but the reported skull stiffness values for all regions were essentially zero at resonance frequencies (Table 4).

Franke[24] performed mechanical impedance tests between 200Hz and 1600Hz on various human specimens. It was determined that a dry, eviscerated human skull had a higher resonance frequency than that of a skull filled with gelatin. Tests were also performed on live subjects and cadavers. While bone vibration was not detected in the live human subjects, the resonance frequency of the cadaver heads was at 900Hz. Stiffness values at resonance for all subjects were very close to zero. No antiresonance frequencies or their corresponding stiffness values were reported (Table 4).

Table 4. Results of mechanical impedance studies

Author	Specimen	Skull Region	Antiresonance (Hz)	Stiffness at Antiresonance (N/mm)	Resonance (Hz)	Stiffness at Resonance (N/mm)
Stalnaker et al.[22]	Cadaver	Whole	166	4553	820	Not reported
Hogdson et al.[23]	Cadaver	Frontal	360	26269	950	0
		Side parietal	450	26269	960	0
		Top parietal	300	15761	760	0
		Occipital	180	29772	1100	0
Franke[24]	Dry skull	Whole	-	-	820	0
	Dry skull with gelatin		-	-	500	0
	Live human		No bone vibration detected			
	Cadaver		-	-	900	0

Other studies investigated skull stiffness by conducting impact tests[25,26,28] and drop tests[27]. During the impact tests, the specimen was struck by an impactor under various conditions[25,26,28]. For the study that performed drop tests[27], the skull was dropped from predetermined heights onto a force plate. During both types of tests[25-28], the force exerted on the

skull and the amount of skull deflection were measured. These data were used to generate force-deflection curves from which skull stiffness values were determined. Force-deflection curves often exhibit a nonlinear toe region in which the skin deflects first and then the skull. Most of the studies reviewed in the current study did not include this region for skull stiffness calculations but used only the linear portion of the curve (Figure 1).

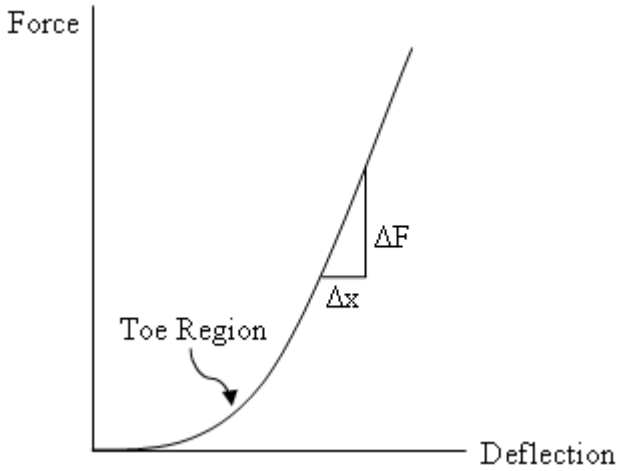

Figure 1. Typical force-deflection curve.

Allsop et al.[25] measured force-deflection characteristics of the temporo-parietal region of the skull on thirty-one cadaver heads, including the skin and intracranial contents. Cadaver heads were mounted in plaster and impacted by one of two impactors: a flat, rectangular surface; or a flat, circular impacting surface (Table 5). The impactors were instrumented with force transducers and string potentiometers to measure force on the skull and deflection of the skull, respectively. The rectangular impactor was dropped onto the parietal region of the head from a height of 102cm, which resulted in an impact velocity of 4.3m/s. The circular impactor was dropped onto the temporo-parietal region from a height of 38cm and impacted the head at a velocity of 2.7m/s. Stiffness values were calculated from the linear-most region of the force-deflection curve. The average stiffness was 4200N/mm for impacts with the rectangular impactor and 1800N/mm for impacts with the circular impactor (Table 5).

Yoganandan et al.[26] determined the stiffness characteristics of the entire skull under quasistatic and dynamic loading. Twelve cadaver heads, with the skin and intracranial contents intact, were exposed to loading rates of 2.54mm/s for quasistatic loading and between 7.1mm/s and 8.0mm/s for dynamic loading. All impacts were performed with a hemispherical anvil (Table 5). Several regions of the skull were tested. The force exerted on the skull was measured by a uniaxial force gauge while the deflection of the skull was measured by a linear variable differential transformer. Stiffness values were determined from the linear-most region of force-deflection curves that were generated from collected data. During quasistatic loading, stiffness ranged from 467N/mm to 1290N/mm with an average of 812N/mm. Stiffness ranged from 2462N/mm to 5867N/mm with an average of 4023N/mm for dynamic loading (Table 5).

A second study conducted by Yoganandan et al.[27] investigated the effects of lateral impacts on the skull. Ten cadaver heads, with the skin and intracranial contents intact, were instrumented with triaxial accelerometers to measure skull deflection at the temporo-parietal region contralateral to the impacted side, the anterior region, and the posterior region of the head. The heads were dropped from various heights, with impact velocities between 4.9m/s and 7.7m/s. The skulls were oriented so that the temporo-parietal region of the skull impacted a padded force platform which was instrumented with a six-axis load cell to measure the force exerted on the skull (Table 5). Acceleration and force data were used to obtain skull stiffness characteristics. In this study, skull stiffness was calculated using the peak force and deflection. The average skull stiffness measured was 562N/mm (Table 5).

A study conducted by Cormier et al.[28] investigated frontal bone impact and stiffness. Twenty-seven fresh, unembalmed male cadaver heads, including the skin and intracranial contents, were exposed to forty-six impacts with a rigid cylindrical impactor. The impact speed

was 5.3m/s. Force exerted on the skull was measured by a load cell. Two uniaxial accelerometers were used to measure the deflection of the skull. Stiffness values were calculated from the linear-most region of the force-deflection curve. The average stiffness of the frontal bone was reported to be 475N/mm (Table 5).

Table 5. Skull stiffness values determined by impact and drop tests.

Author	Skull Impact Region	Average Stiffness [Minimum-Maximum] (N/mm)	Test Setup
Allsop et al[25]	Parietal, rectangular impactor	4200 [1600-6430]	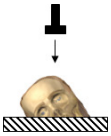
	Temporo-parietal, circular impactor	1800 [700-4760]	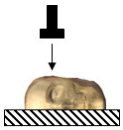
Yoganandan et al[26]	Quasistatic: average of top, parietal, temporal, frontal, occipital	812 [467-1290]	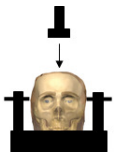
	Dynamic: average of top, parietal, temporal, frontal, occipital	4023 [2462-5867]	
Yoganandan et al[27]	Temporo-parietal	562 [390-689]	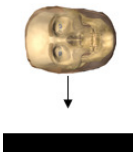
Cormier et al[28]	Frontal	475 [not specified]	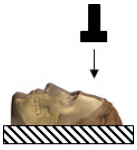

Evaluation of Cranial Movement

Skull stiffness values were used to calculate the amount of external force required to induce cranial motion in human specimens (Table 6). Only the human specimens in cranial movement studies were of concern because the stiffness values were evaluated using the human skull. Heifetz et al.[21] was the only one to report measures of cranial movement in human specimens. Therefore, cranial motion measurements from this study were used to determine whether measurements of cranial motion were reasonable in human specimens as a result of CO.

Table 6. Force necessary to cause cranial motion measured in Heifetz human study

		Case 1: 3.72µm of deflection	**Case 2: 0.78µm of deflection**
Study	**Stiffness Type**	**Required Force (N)**	
Stalnaker et al[22]	Whole skull	16.98	3.55
Hogdson et al[23]	Frontal	97.72	20.49
	Side Parietal	97.72	20.49
	Top Parietal	58.63	12.29
	Occipital	110.75	23.22
Allsop et al[25]	Temporo-prietal (rect)	15.62	3.28
	Temporo-parietal (circ)	6.70	1.40
Yoganandan et al[26, 27]	Quasistatic (average of several regions)	3.02	0.63
	Dynamic (average of several regions)	21.83	4.58
	Temporo-parietal	2.09	0.44
Cormier et al[28]	Frontal	1.78	0.37

Discussion

The purpose of this study was to review findings of cranial movement in animal and human specimens and evaluate the validity of cranial movement due to manual manipulation in humans through engineering analysis. Several studies reported quantitative and qualitative results of cranial movement. In these studies, cranial motion was induced by various internal and external

stresses on the cranium. A wide range of cranial motion was seen across animal and human specimens. Engineering analysis was conducted on these findings to determine whether measurements of cranial motion were reasonable in human specimens as a result of CO.

Skull stiffness values were used to calculate the amount of external force required to induce cranial motion in human specimens. Pitlyk et al.[17] reported no quantitative measurements in cranial motion. Therefore, no forces could be calculated from that study. Heifetz et al.[21] reported small cranial movements, 0.78μm and 3.72μm, due to increases in intracranial pressure in two comatosed patients. The forces equivalent to the intracranial pressure increases in the two subjects ranged from 0.438N to 23.2N for cranial movement of 0.78μm and 2.09N to 111N for cranial movement of 3.72μm.

Studies have been conducted to determine the amount of pressure exerted during CO. A study by Parodi et al.[29] measured the pressure exerted by two groups of osteopathic students during CO. One group received instructions for palpation while the other did not. Pressures were measured by a 0.71-cm^2 force sensor placed on the left side of the patient's frontal bone. Students were asked to place their index finger in the sensor during palpation. Palpation pressures ranged from 0.19 N/cm^2 to 1.12N/cm^2 corresponding to forces between 0.13N and 0.80N. A second study[30] quantified pressures exerted by twenty-three students and one experienced physician during palpation of the cervical spine. A force sensor with a surface area of 0.2cm^2 was attached to each subject's index finger during palpation. Pressures ranged from 4.0N/cm^2 to 41.0N/cm^2 corresponding to forces between 0.8N and 8.2N.

Many of the forces calculated in the current study are much larger than those measured during CO. However, the studies investigating the amount of pressure applied during CO took measurements from only one finger. Osteopathic physicians typically use more than one finger

during manual manipulation. Therefore, the total amount of pressure applied to the skull during CO should be greater than the pressures reported in the palpation studies. While the amount of cranial motion may vary by subject and the region of the head on which forces are applied, it is reasonable that small amounts of cranial motion may occur during CO.

There are limitations in the current study that should be addressed. The accuracy of the reported measurements of cranial motion must be considered. The forces quantified in the current study are based on only two subjects in whom very small amounts of cranial motion were measured[21]. In addition, the strain gauges used to measure cranial motion on those subjects measured changes across the diameter of the head. Therefore, measurements reported by Heifetz et al.[21] may not be motion at the cranial sutures but deflection of the skull between the sutures. Also, the validity of these measurements is of concern as cranial motion values are very small. Such measurements would require extremely sensitive strain gauges and an extremely stiff test apparatus. Since little is known about the strain gauges used in the study, the accuracy and sensitivity of those strain gauges could not be assessed.

The relevance of this study to CO should be considered. Many of the cranial motion investigations reviewed in the current study involve expansion of the skull while CO involves compression of the skull. Although CO has been proven to be successful in treating symptoms of medical and neurological problems, the underlying physiological mechanisms of CO must be investigated, specifically the correlation between cranial motion and the effectiveness of CO. There is no existing evidence as to whether cranial motion contributes to the reduction in symptoms that results from CO. Patient improvement may be attributed to several different mechanisms such as: a placebo effect, relaxation of muscles due to massaging effects, or

decrease in pressure on the cranial nerves due to massaging. Therefore, further research should be conducted to investigate the effects of cranial motion in CO.

Further investigation of cranial motion can be done through computational modeling. Finite element modeling of various body parts has dramatically advanced over the past few years. Models currently exist to assess the risk of eye injury[31], the risk of injury to pregnant occupants in automobile collisions[32,33]. Others models can determine the risk of specific injuries that may result from vehicle collisions, such as blunt carotid injury[34], pulmonary contusion[35,36], and rib fracture[37]. Existing head models[38-43] assess head injury under several different conditions such as whiplash and direct impact. All of these models have helped to better understand injury mechanisms and are critical tools in injury biomechanics.

Conclusions

In this study, cranial movement in animal and human specimens was reviewed. In addition, the validity of cranial movement due to manual manipulation in humans was evaluated through engineering analysis. A wide range of cranial motion was reported across several specimens. Previously reported skull stiffness values were used to calculate the amount of external force required to induce cranial motion in human specimens. Cranial motion measurements in humans ranged from zero to 3.72μm, requiring equivalent forces between 0.44N and 111N on the cranium. Studies that have determined the forces applied by a single finger during CO have measured forces ranging from 0.13N to 8.2N. Osteopathic physicians typically use more than one finger during manual manipulation. Therefore, the total force exerted on the skull during CO should be greater. While the amount of cranial motion may vary by subject and skull region of the head on which forces are applied, it is reasonable that small amounts of cranial motion may occur during CO. However, it should be noted that there is no existing evidence as to

whether cranial motion contributes to the reduction in symptoms that results from CO. Patient improvement may be attributed to several different mechanisms such as: a placebo effect, relaxation of muscles due to massaging effects, decrease in pressure on the cranial nerves. Therefore, further research should be conducted to investigate the effects of cranial motion in CO.

References

1. Shain K, Madigan ML, Rowson S, Bisplinghoff J, Duma SM. Analysis of the ability of catcher's masks to attenuate head accelerations on impact with a baseball. *Clinical Journal of Sport Medicine* 2010; 20(6):422-27.

2. Duma SM, Rowson S. Past, present, and future of head injury research. *Exercise and Sport Sciences Reviews* 201; 39(1):2-3.

3. Duma SM, Manoogian SJ, Bussone W, Brolinson PG, Goforth MW, Donnenwerth JJ, et al. Analysis of real-time head accelerations in collegiate football players. *Clinical Journal of Sports Medicine* 2005; 15(1):3-8.

4. Rowson S, Brolinson PG, Goforth MW, Dietter D, Duma SM. Linear and angular head accelerations measurements in collegiate football. *Journal of Biomechanical Engineering 2009;* 131(6):061016.

5. Crisco JJ, Fiore R, Beckwith JG, Chu JJ, Brolinson PG, Duma S, et al. Head Impact Exposures in Individual Collegiate Football Players. *Journal of Athletic Training* 2010; 45(6):549-559.

6. Duma SM, Crandall JR, Rudd RW, Kent RW. Small female head and neck interaction with a deploying side airbag. *Accidental Analysis and Prevention* 2003; 35(5):811-816.

7. Manoogian SJ, Kennedy EA, Wilson KA, Duma SM, Alem NM. Predicting Neck Injuries Due to Head-Supported Mass. *Aviation, Space, and Environmental Medicine* 2006; 77(5):509-514.

8. Frymann VM, Carney RE, Springall P. Effect of osteopathic medicine on neurologic development in children. *Journal of the American Osteopathic Association* 1992; 92(6):729-744.

9. Hayden C, Mullinger B. A preliminary assessment of the impact of cranial osteopathy for the relief of infantile colic. *Complementary Therapies in Clinical Practices* 2006; 12:83-90.

10. Joyce P, Clark C. The Use of CranioSacral Therapy To Treat Gastroesophageal Reflux in Infants. *Infants and Young Children* 1996; 9(2):51-57.

11. Sandhouse ME, Shechtman D, Sorkin R, Drowos, JL, Caban-Martinez AJ, Patterson MM, et al. Effect of Osteopathy in the Cranial Field on Visual Function – A Pilot Study. *Journal of the American Osteopathic Association* 2010; 110(4):239-243.

12. Barke L, Gelman S, Lipton JA. A successful use of cranial-sacral osteopathy in the treatment of post-traumatic headache following subarachnoid hemorrhage. *American Academy of Osteopathy Journal* 1997:22-23.

13. King HH. Osteopathy in the Cranial Field. In: Chila, Anthony G. *Foundations of Osteopathic Medicine, Third Edition*. Baltimore MD: Lippincott Williams & Wilkinson; 2011, p. 728-48.

14. Moran RW, Gibbbons P. Intraexaminer and Interexaminer Reliability for Palpation of the Cranial Rhythm Impulse at the Head and Sacrum. *Journal of Manipulative and Physiological Therapeutics* 2001; 183-90.

15. Wirth-Pattullo V, Hayes KW. Interrater Reliability of Craniosacral Rate Measurements and Their Relationship with Subjects' and Examiners' Heart and Respiratory Rate Measurements. *Physical Therapy* 1994; 908-16.

16. Michael DK, Retzlaff EW. A preliminary study of cranial bone movement in the squirrel monkey. *Journal of the American Osteopathic Association* 1975; 866-69.

17. Pitlyk PJ, Piantanida TP, Ploeger DW. Noninvasive intracranial pressure monitoring. *Neurosurgery* 1985; 581-84.

18. Oudhof HA, van Doorenmaalen WJ. Skull morphogenesis and growth: Hemodynamic influence. *Acta Anatomica* 1983; 181-86.

19. Downey PA, Barbano T, Kapur-Wadhwa R, Sciote JJ, Siegel MI, Mooney MP. Craniosacral therapy: The effects of cranial manipulation on intracranial pressure and cranial bone movement. *Journal of Orthopaedics and Sports Physical Therapy* 2006; 845-853.

20. Adams T, Heisey RS, Smith MC, Briner BJ. Parietal bone mobility in the anesthetized cat. *Journal of the American Osteopathic Association* 1992; 599-622.

21. Heifetz MD, Weiss M. Detection of skull expansion with increased intracranial pressure. *Journal of Neurosurgery* 1981; 811-12.

22. Stalnaker RL, Fogle JL, McElhaney JH. Driving Point Impedance Characterisitcs of the Head. *Journal of Biomechanics* 1971; 4:127-139.

23. Hodgson VR, Gurdjian ES, Thomas LS. The Determination of Response Characteristics of the Head with Emphasis on Mechanical Impedance Techniques. *Eleventh Stapp Car Crash Conference*. New York: Society of Automotive Engineers, Inc., 1967. 125-38.

24. Franke EK. Response of the Human Skull to Mechanical Vibrations. *The Journal of the Acoustical Society of America* 1956; 28(6):1277-84

25. Allsop DL, Perl TR, Warner CY. Force/Deflection and Fracture Characteristics of the Temporo-parietal Region of the Human Head. *35th Stapp Car Crash Conference*. San Diego, California: Society of Automotive Engineers, 1991.

26. Yoganandan N, Pintar FA, Sances A, Walsh PR, Ewing CL, Thomas DJ, et al. Biomechanics of Skull Fracture. *Journal of Neurotrauma* 1995; 659-68.

27. Yoganandan N, Zhang J, Kuppa S, Eppinger RH. Biomechanics of Lateral Skull Fracture. *International Research Council on the Biomechanics of Impact*. Lisbon, Portugal, 2003. 69-78.

28. Cormier J, Manoogian S, Bisplinghoff J, Rowson S, Santago A, McNally C, et al. The tolerance of the frontal bone to blunt impact. *Journal of Biomechanical Engineering* 2011; 133(2):021004.

29. Zegarra-Parodi R, de Chauvigny de Blot P, Rickards LD, Renard E. Cranial Palpation Pressures Used by Osteopathic Students: Effects of Standardized Protocol Training. *Journal of the American Osteopathic Association* 2009; 109(2):79-85.

30. Marcotte J, Normand MC, Black P. Measurement of the Pressure Applied During Motion Palpation and Reliability for Cervical Spine Rotation. *Journal of Manipulative Medicine and Physiological Therapeutics* 2005; 28(8):591-96.

31. Weaver AA, Loftis KL, Tan JC, Duma SM, Stitzel JD. CT Based Three-Dimensional measurement of Orbit and Eye Anthropometry. *Investigative Ophthalmology & Visual Science* 2010; 51(10):4892-4897.

32. Moorcroft DM, Stitzel JD, Duma GG, Duma SM. Computation model of the pregnant occupant: predicting the risk of injury in automobile crashes. *American Journal of Obstetric and Gynecology* 2003; 189(2):540-544.

33. Moorcroft DM, Stitzel JD, Duma SM, Duma GG. The effects of uterine ligaments on the fetal injury risk in frontal automobile crashes. *Journal of Automobile Engineering* 2003; 217(D):1049-1055.

34. Gayzik FS, Bostrom O, Ortenwall P, Duma SM, Stitzel JD. An experimental and computational study of blunt carotid artery injury. *Annals of Advanced Automotive Medicine* 2006; 50:13-32.

35. Gayzik FS, Shayn MR, Gabler HC, Hoth JJ, Duma SM, Meredith JW, et al. Characterization of Crash Induced Thoracic Loading Resulting in Pulmonary Contusion. *Journal of Trauma* 2009; 66(3):840-849.

36. Stitzel JD, Gayzik FS, Hoth JJ, Mercier J, Gage HD, Morton KA, et al. Development of a finite element-based injury metric for pulmonary contusion part I: model development and validation. *Stapp Car Crash Journal* 2005; 49:271-289.

37. Stitzel JD, Baretta JT, Duma SM. Predicting Fracture due to blunt impact: a sensitivity analysis of the effects of altering failure strain of human cortical rib bone. *International Journal of Crashworthiness* 2004; 9(6):633-642.

38. Turquier F, Kang HS, Trosseille X, Willinger R, Lavaste F, Tarriere C, et al. Validation Study of a 3D Finite Element Head Model Against Experimental Data. *Society of Automotive Engineers* 1996

39. Zhang L, Yang KH, Dwarampudi R, Omori K, Li T, Chang K, et al. Recent Advances in Brain Injury Research: A New Head Model Development and Validation. *Stapp Car Crash Journal* 2001; 45:375-400.

40. Takhounts EG, Eppinger RH, Campbell JQ, Tannous RE, Power ED, Shook LS. On the Development of the SIMon Finite Element Head Model. *Stapp Car Crash Journal* 2003; 47:107-133.

41. Takhounts EG, Ridella SA, Hasija V, Tannous RE, Campbell JQ, Malone D, et al. Investigation of traumatic brain injury using the next generations of simulated injury monitor (SIMon) finite element head model. *Stapp Car Crash Journal* 2008; 52:1-31.

42. Stemper BD, Yoganandan N, Pintar FA. Validation of a head-neck computer model for whiplash simulation. *Medical and Biological Engineering and Computing* 2004; 2:333-338.

43. Zong Z, Lee HP, Lu C. A three-dimensional human head finite element model and power flow in a human head subject to impact loading. *Journal of Biomechanics* 2004; 39:284-292.

CHAPTER 2

DUMMY AND HUMAN SURROGATE OCCUPANT HEAD KINEMATICS: A COMPARISON OF DATA COLLECTION METHODOLOGIES

The assessment of occupant response in vehicle collisions is important for advancements in occupant restraints. Several data collection methodologies exist for quantifying occupant kinematics: Vicon motion analysis, high-speed video analysis, and linear accelerometers and angular rate sensors. While Vicon systems are accurate and require minimal post-processing, they are costly. High-speed video analysis is more cost effective than Vicon systems but tedious and time-consuming. Data acquisition using accelerometers and angular rate sensors is relatively inexpensive, but the accuracy of using data from such sensors to quantify global occupant displacement requires further investigation. Therefore, the purpose of this study is to evaluate the accuracy of calculating head trajectories of Hybrid III dummies and post mortem human surrogates from linear acceleration and angular rate data by comparing calculated head trajectories to head trajectories quantified using motion capture data. Head trajectories obtained from motion capture data and sensor data were plotted up to maximum forward excursion of the head for eight frontal sled tests. Although, trajectories calculated from sensor data did not exactly match motion capture data, they were found to be reasonable estimates of head motion. The average percent difference of maximum forward excursion of all eight tests was 12.01(± 10.30%). It was found that accelerometer data overestimated maximum forward excursion in all but two tests. The results of this study indicate that data collection via accelerometers produces similar results to data collection from motion analysis. However, caution should be exercised during interpretation of accelerometer data.

Keywords: head, trajectory, kinematics, motion analysis, accelerometer, biomechanics

Introduction

Injuries to the head and neck can occur during automobile collisions (Duma et al. 2003). Direct contact between the head and the vehicle interior in a frontal crash can result in facial fractures (Cormier and Duma 2009), eye injuries (Duma et al. 2000, 2002), traumatic brain injuries (Funk et al. 2007), and damage to the cervical spine (Duma 2008). Studies have shown that the use of safety restraints, such as seat belts and airbags help reduce the risk of these injuries (Duma et al. 2005; Cormier and Duma 2009). Occupant safety is of primary interest in the automobile industry. Therefore, vehicle crash tests are conducted to assess occupant safety. Occupant kinematic data from these tests can be used to assess the likelihood of contacting components of the vehicle interior for both restrained and unrestrained occupants.

Several data collection methodologies exist for quantifying occupant kinematics during a collision event. Some of these methodologies include: Vicon motion analysis (Beeman et al. 2011), high-speed video analysis (Bolton et al. 2006, Padgaonkar et al. 1975, Chou and Sinha 1976, Shea and Viano 1994), and the use of accelerometers and angular rate sensors (Beeman et al. 2011, Bolton et al. 2006, Padgaonkar et al. 1975, Chou and Sinha 1976, Shea and Viano 1994). While Vicon systems are extremely accurate and involve minimal post-processing, they are costly. High-speed video analysis is more cost effective than Vicon systems. However, this methodology is laborious and time-consuming. Data acquisition using accelerometers and angular rate sensors is relatively inexpensive, but the accuracy of using acceleration and angular rate data to quantify global occupant displacement in full scale sled tests has not been determined. If proven to be accurate, accelerometers and angular rate sensors could provide a simpler, more cost effective method for quantifying occupant kinematics in vehicle collisions.

Studies have been conducted to assess the effectiveness of data collection using sensors. Some studies have investigated the effectiveness of noninvasive data collection in the field, such as the investigation of human factors and ergonomics in the work place (Edmison et al. 2004; Hakkarainen et al. 2010). Other compared methods of quantifying angular rates and accelerations of a rigid body (Padgaonkar et al. 1975, Chou and Sinha 1976). A study by Shea and Viano (1994) investigated the accuracy of using linear accelerometer data to calculate the angular rotation and trajectory of a Hybrid III (HIII) head in mini- and full-scale sled tests. However, these studies were all performed under controlled conditions. The purpose of this study is to evaluate the accuracy of calculating head trajectories of HIII and post mortem human surrogates (PMHS) from linear acceleration and angular rate data by comparing calculated head trajectories to head trajectories obtained from motion capture data in full scale sled tests.

Methods

Global trajectory data and sensor data, i.e. accelerations and angular rates, were obtained for two series of high-speed, frontal sled tests. One series was conducted at Virginia Tech (VT) (Beeman et al. 2011) while the other was conducted at the University of Virginia (UVA) (Bolton et al. 2006).

In the first test series, four 40-kph frontal sled tests were conducted at VT with three 50th percentile PMHS and one 50th percentile male HIII (Beeman et al. 2011). The sled pulse was a 28.6-G pulse taken from the FMVSS 208 standard crash test for a 2007 Toyota Camry. The test buck included a steering column and a rigid seat. The occupants were restrained by a driver side 3-point belt with a 5-kN load limiter. Kinematic data for the head were collected with three single-axis linear accelerometers (x,y,z), and a three-axis angular rate sensor ($\omega_x, \omega_y, \omega_z$) rigidly mounted to the top of the head. A Vicon motion analysis system was also used to quantify the 3D kinematics of retroreflective markers placed on the head. The markers were then used to determine the 3D trajectories of the head CG. A common reference for the CG of the head is the Frankfort plane which passes through the inferior rims of the ocular orbits and superior edges of the auditory meatus (Bussone et al. 2005). In addition, the CG of the head lies in the mid-sagittal plane of the head. For the VT study, the head CG was approximated to be at the antero-superior aspect of the helix of the ear.

The data from four 48-kph tests conducted at the UVA, two PMHS and two HIII 50th percentile subjects, were obtained (Bolton et al. 2006). The test buck included the front vehicle interior of a 1997 Ford Taurus. Occupants were placed in the right front passenger seat of the test buck. Restraints included a standard 3-point belt and a depowered airbag, which has reduced inflation power to reduce the risk of injury (Duma et al. 2005). Similar to the VT test series,

three single-axis linear accelerometers and one three-axis angular rate sensor rigidly mounted to the head were used to quantify head kinematics (Bolton et al. 2006). Acceleration and angular rate data were obtained from the National Highway Traffic Safety Administration (NHTSA) signal browser software (test #8380-8383). High-speed video analysis was also performed to obtain head x-z motion data by tracking a photo target aligned with the lateral aspect of the head CG. However, the location of the head CG was not specified in the report for the UVA tests. The head x-z motion data were digitized from plots in the NHTSA report for this test series (Bolton et al. 2006). Table 7 summarizes subject information and restraints of the eight tests from which data was obtained (Beeman et al. 2011 and Bolton et al. 2006). In the restraint columns (last three columns), an "x" indicates the presence of a restraint.

Table 7. Subject and restraint information for frontal sled tests.

	Test ID	NHTSA ID	Subject Type	Gender	Stature *(cm)*	Weight *(kg)*	Age *(yr)*	Airbag	Pretensioner	Load Limiter
VT series	PMHS 1	N/A	PMHS	M	174	74.3	51			x
	PMHS 2	N/A	PMHS	M	176	68.6	63			x
	PMHS 3	N/A	PMHS	M	184	86.4	79			x
	HIII	N/A	HIII 50th	M	175	78.0	N/A			x
UVA series	UVA 665	8382	PMHS	M	176	85.3	55	x		
	UVA 666	8383	PMHS	M	176	83.9	69	x		
	UVA 663	8380	HIII 50th	M	175	78.0	N/A	x		
	UVA 664	8381	HIII 50th	M	175	78.0	N/A	x		

Figure 2 shows the general steps for processing the acceleration and angular rate data to calculate the trajectory of the head during a frontal impact. All data were filtered according to SAE standards, i.e. acceleration data were filtered using CFC180 and angular rate data were filtered using CFC60 (Beeman et al. 2011). If necessary, acceleration data were transformed to the head CG. Then the acceleration data were adjusted for angular rotation followed by double integration of the accelerations to find displacements. Finally, head displacement relative to the test buck was found in the x-direction.

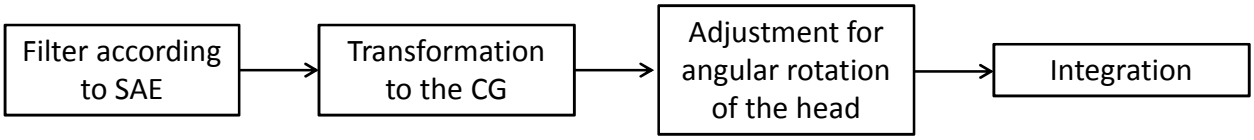

Figure 2.General procedure for obtaining head trajectory from acceleration and angular rate data.

Transformation of the acceleration data to the head CG was important for tests in which sensors were not mounted at the head CG, such as the tests with a PMHS. Acceleration data from test dummies did not need to be transformed to the CG because the sensors were mounted at the head CG. Acceleration in the y-direction was not transformed because the head trajectory in the x-z plane was of primary interest. Equation 1 shows the transformation of the acceleration in the x-direction to the CG. Equation 2 shows the transformation of the acceleration for the z-direction to the CG (Naunheim et al. 2003). The transformed accelerations ($a_{x,CG}$ and $a_{z,CG}$) depend on the original acceleration (a_x and a_z), angular accelerations (α_x, α_y, and α_z), angular rates (ω_x, ω_y, and ω_z), and the distances between the CG and the location of the sensor (X, Y, and Z). Figure 3 illustrates the distances X and Z. For this study, the distance Y was assumed to be zero.

$$a_{x,CG} = a_x - (Z\alpha_y - Y\alpha_z) - \omega_x(Z\omega_z + Y\omega_y) + X(\omega_y^2 + \omega_z^2) \quad (1)$$

$$a_{z,CG} = a_z - (X\alpha_y - Y\alpha_x) - \omega_z(X\omega_x + Y\omega_y) + Z(\omega_x^2 + \omega_z^2) \quad (2)$$

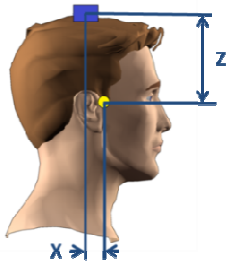

Figure 3. The distances between the sensor and the head CG defined by X and Z.

Since the coordinate system of each accelerometer is local to the sensor, the orientations of the axes change as the head moves throughout a test (Figure 4). However, the linear acceleration data can be transformed from the local coordinate system of the sensor to the global coordinate system by accounting for angular motion. Adjustments for angular rotation in the x- and z- directions are given by Equations 3 and 4, respectively (Shea and Viano 1994). For these equations, lateral motion of the head (y-direction) was assumed to be negligible. Adjusted accelerations (A_x and A_z) are dependent upon the unadjusted accelerations at the CG ($a_{x,CG}$ and $a_{z,CG}$) and the angle β (Figure 5). The angle β is defined as the angular position of the head relative to the frontal plane where a positive angle is counterclockwise from the plane. The angle β was obtained by integrating the angular rate (ω_y) of the head.

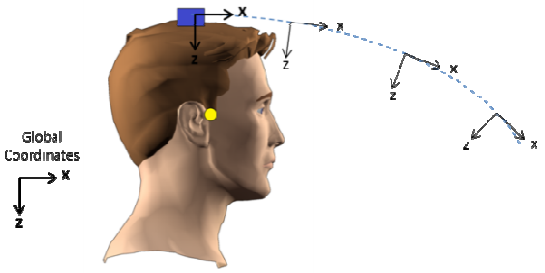

Figure 4. The orientation of the coordinate system changes as the head moves throughout a test.

$$A_X = a_x \cos(\beta) + a_z \sin(\beta) \quad (3)$$

$$A_Z = a_z \cos(\beta) - a_x \sin(\beta) \quad (4)$$

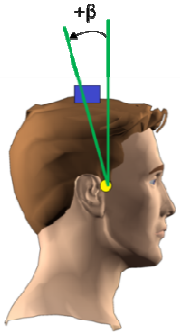

Figure 5. Angular position of the head relative to the frontal plane.

Finally, the acceleration time histories were double integrated to obtain displacements of the sled in the x-direction, the head in the x-direction, and the head in the z-direction (Equation 5). The motion of the head relative to the sled in the x-direction was found by subtracting the displacement of the sled from the displacement of the head (Equation 6).

$$\iint_0^t a(t)\ dt = x(t) \tag{5}$$

$$x_{head/sled} = x_{head,x} - x_{sled,x} \tag{6}$$

After calculating the head trajectories, the maximum forward excursions for the motion capture data, i.e. Vicon or high-speed video analysis data, and the processed accelerometer data were recorded and the percent difference (*PD*) between the two was calculated for each test (Equation 7). In Equation 7, x_{acc} is the maximum forward excursion for the head trajectory calculated from the acceleration data and x_{motion} is the maximum forward excursion of the head obtained from the motion capture data. Therefore, the percent difference will be positive if the calculated maximum excursion is greater than the maximum excursion from motion data.

$$PD = 100 * \frac{x_{acc} - x_{motion}}{x_{motion}} \tag{7}$$

Results

Head trajectories from the motion capture and sensor data obtained from each test were plotted together for comparison. Figure 6 through Figure 9 show the head trajectories for the VT test series. Figure 10 through Figure 13 show trajectories for the UVA series.

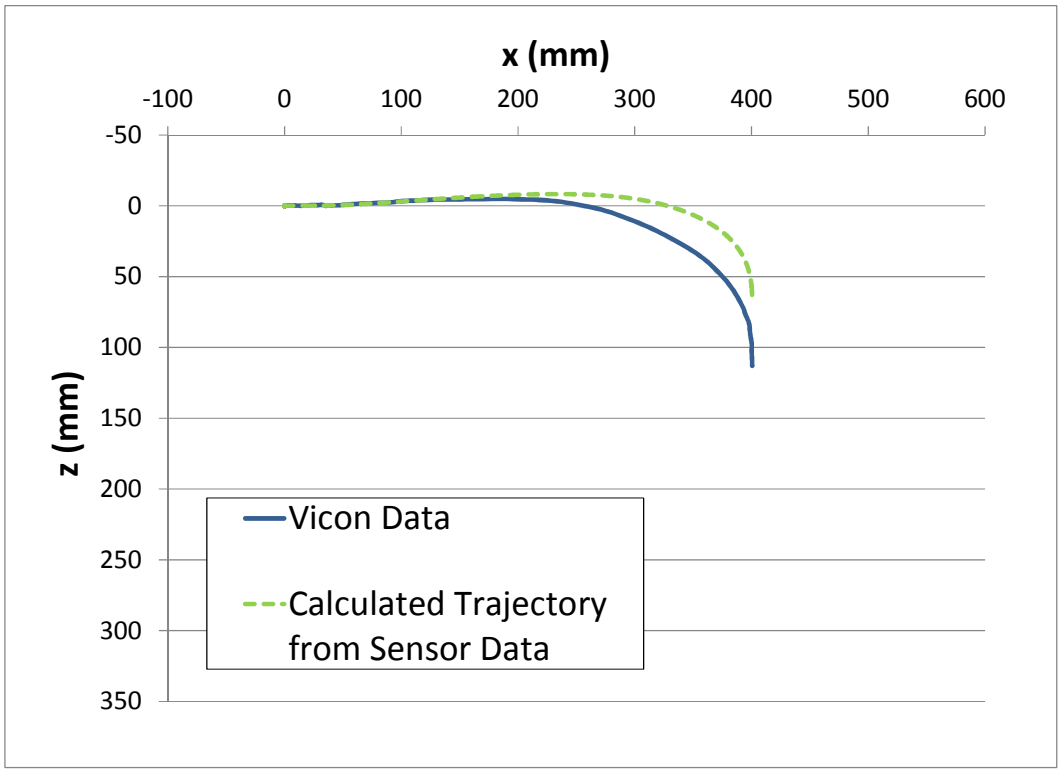

Figure 6. Head trajectories for VT PMHS 1.

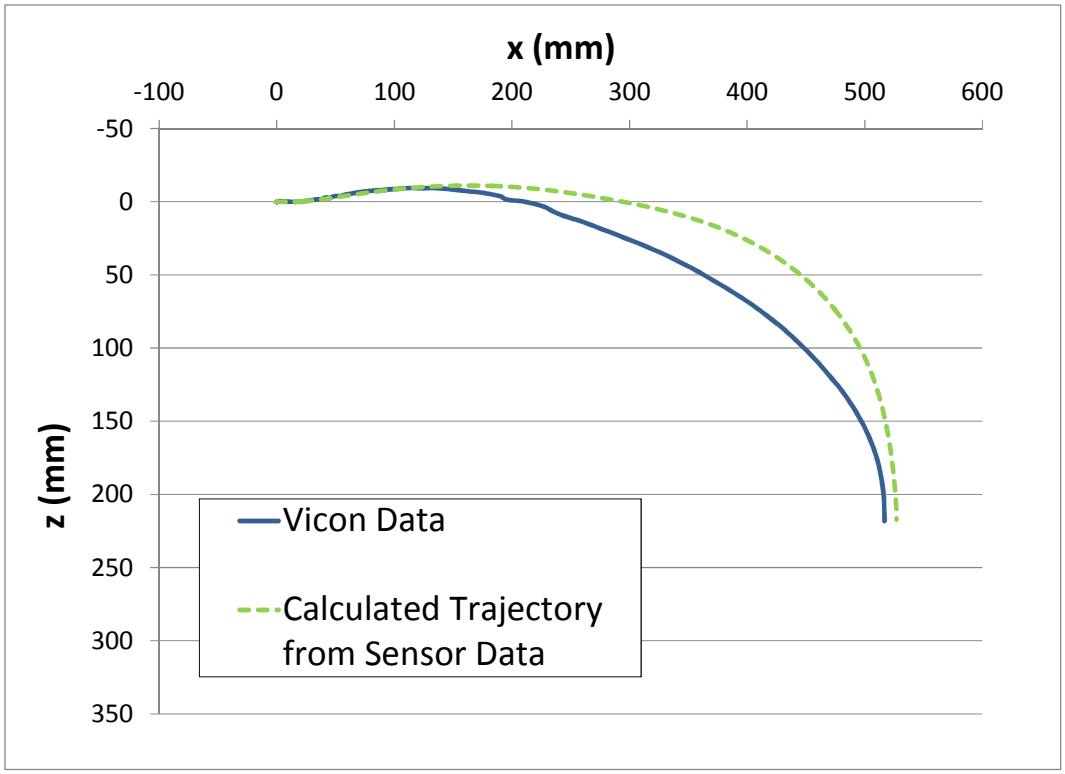

Figure 7. Head trajectories for VT PMHS 2.

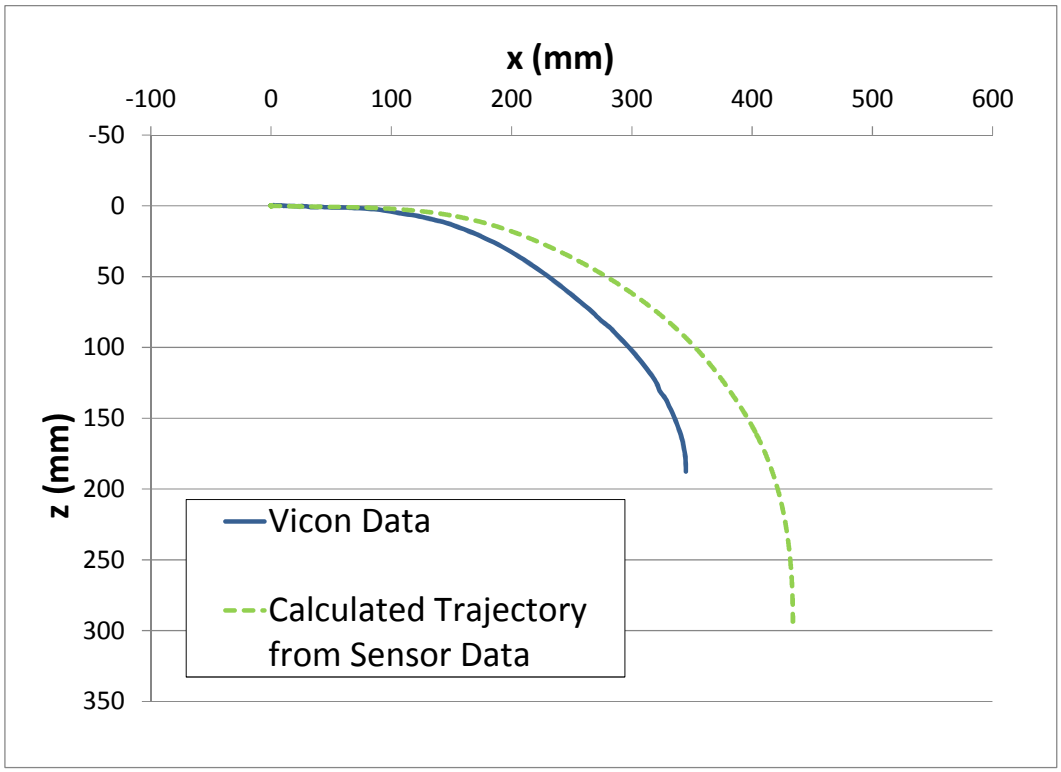

Figure 8. Head trajectories for VT PMHS 3.

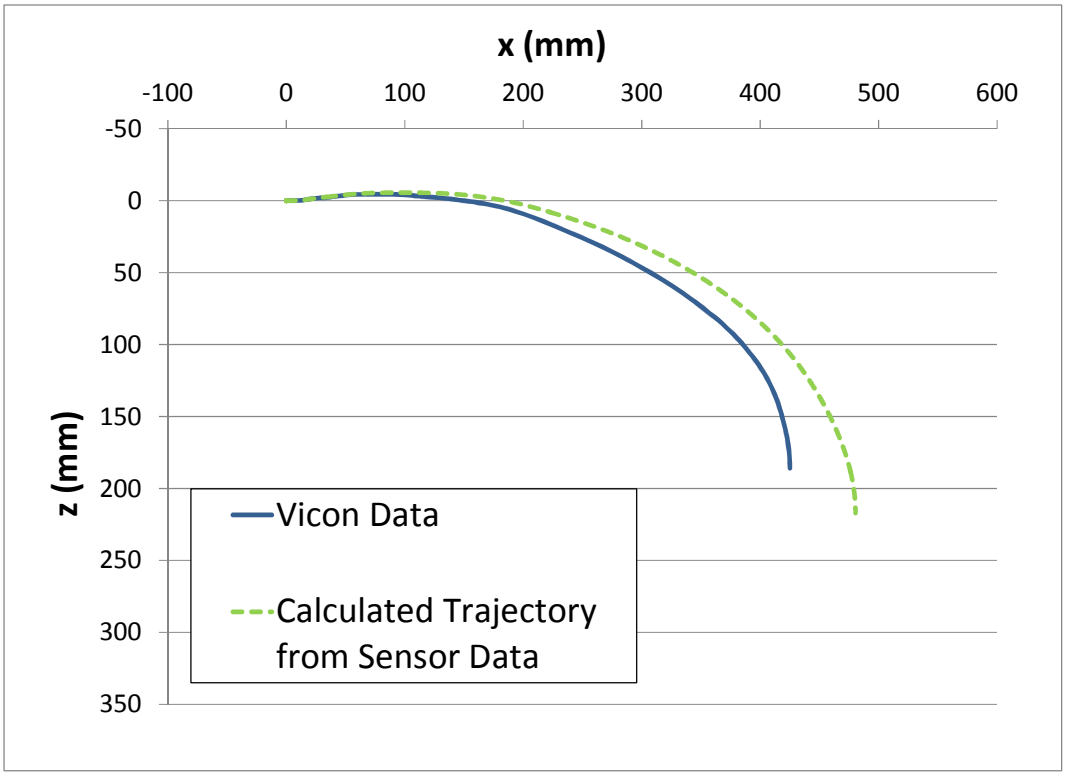

Figure 9. Head trajectories for VT HIII.

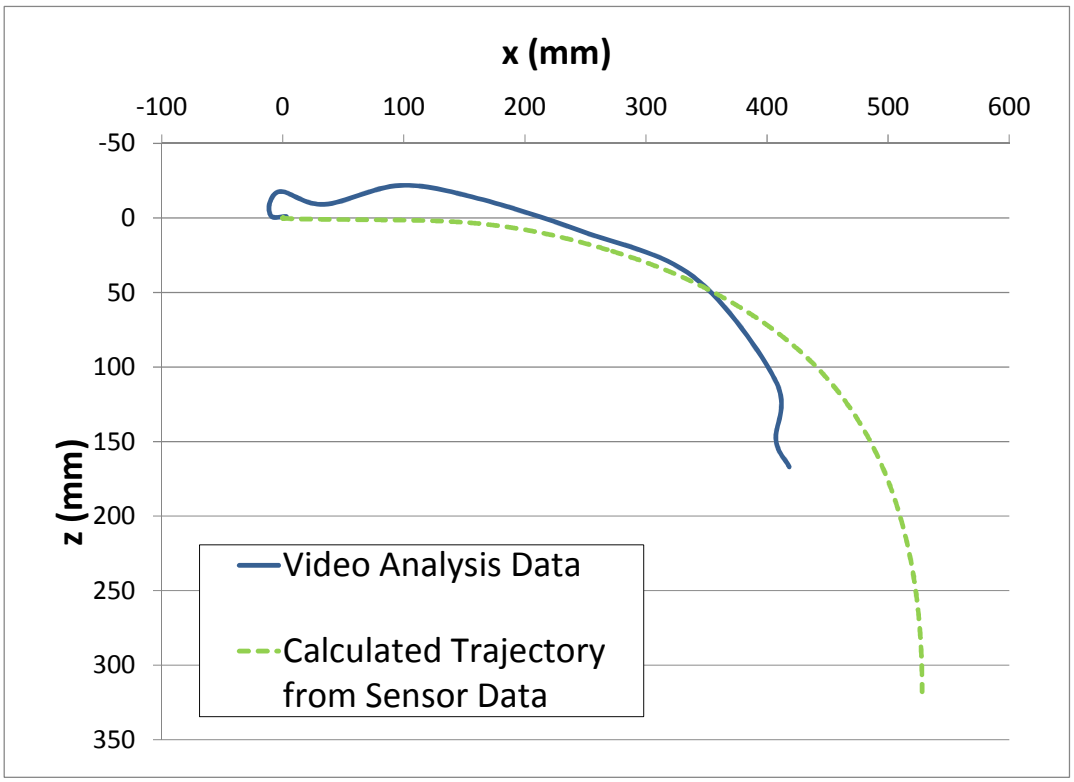

Figure 10. Head trajectories for UVA test 8380.

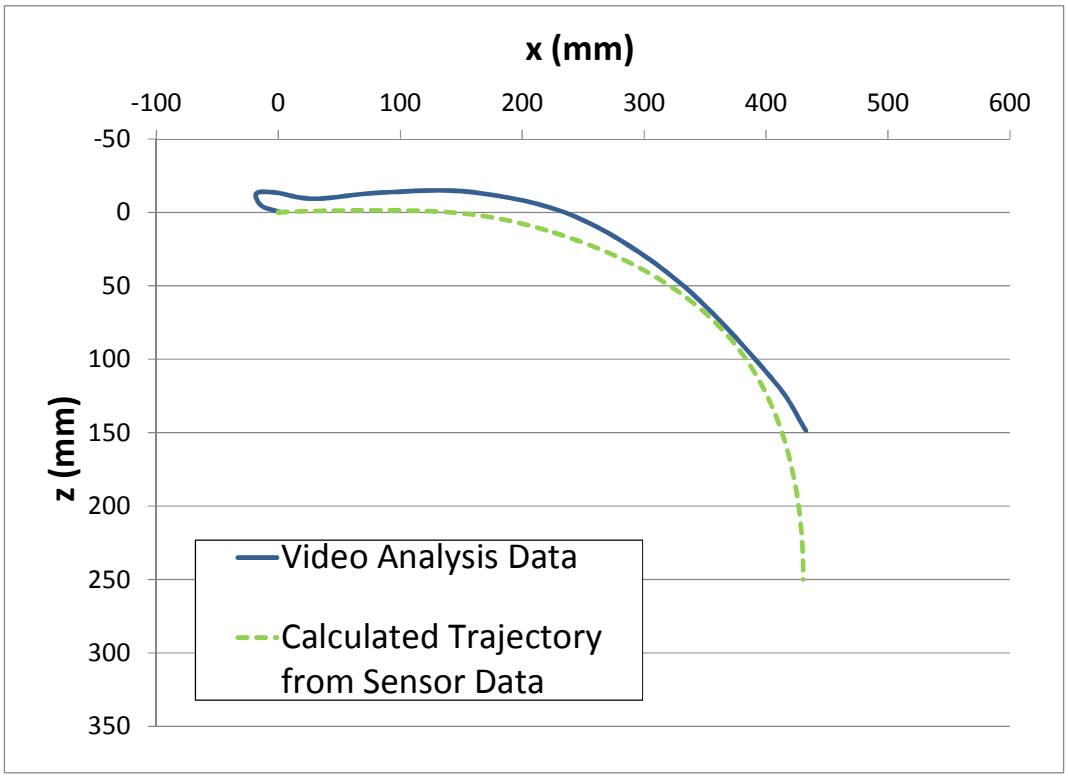

Figure 11. Head trajectories for UVA test 8381.

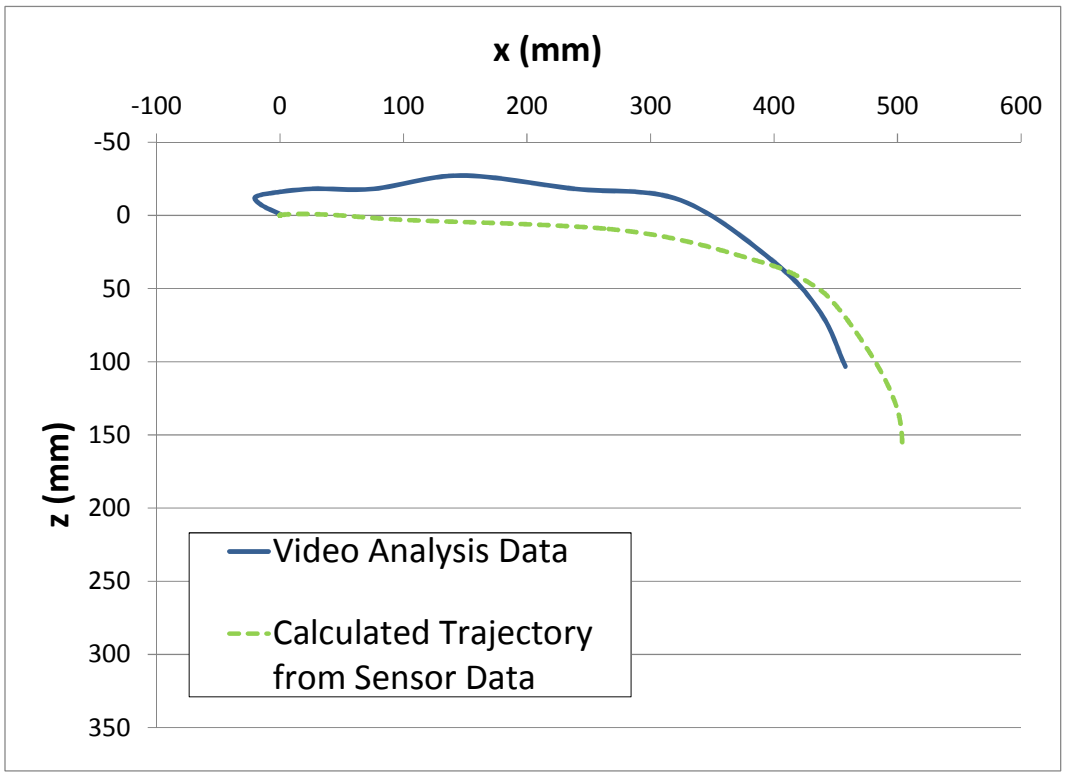

Figure 12. Head trajectories for UVA test 8382.

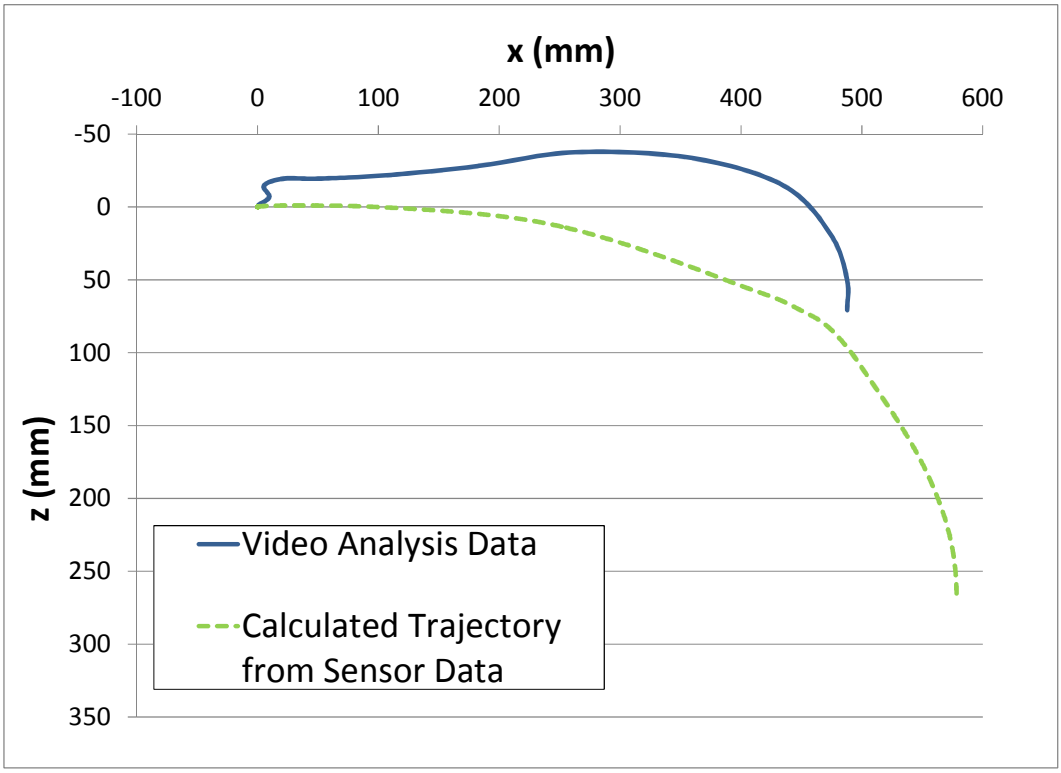

Figure 13. Head trajectories for UVA test 8383.

Maximum forward excursions from the motion capture data and calculated head trajectories from sensor data were compared by calculating the percent difference between the two values (Table 2). A positive percent difference indicates that the maximum forward excursion (x-direction) from the calculated trajectory is greater than that from the motion data.

Table 8. Comparison between motion capture data and calculated forward excursions.

Series	Test ID	Subject Type	Motion Data (x), (mm)	Calculated Forward Excursion (mm)	Percent Difference (%)
VT	**PMHS 1**	PMHS	401	401	0.0
	PMHS 2	PMHS	517	527	2.0
	PMHS 3	PMHS	345	434	25.8
	HIII	HIII	425	480	13.0
UVA	**8380**	HIII	418	528	26.3
	8381	HIII	433	430	-0.6
	8382	PMHS	458	506	10.6
	8383	PMHS	488	581	19.0
				Average	**12.0**
				Standard Deviation	**10.3**

Discussion

In the current study, the accuracy of calculated forward excursion from accelerometer and angular rate sensor data in frontal collisions was assessed relative to motion capture data, i.e. Vicon and video analysis. This was done for eight frontal sled tests, four conducted by VT and four conducted by UVA. Although, trajectories calculated from sensor data did not exactly match motion data, they were found to be reasonable estimates of head motion in a frontal collision. For these tests, the sensor data overestimated forward excursion of the head for all but two tests. The average percent different of all eight tests was 12.01 ± 10.30%, indicating that maximum forward excursion from calculated trajectories were greater than those from motion data. However, this provides a conservative estimate of whether the head will strike a portion of the vehicle interior.

Padgaonkar et al. (1975) performed a validation of a nine-accelerometer scheme and the accuracy of calculating angular accelerations and velocities from the accelerometer data. During the tests, the accelerometer array was mounted in various orientations to a rigid plate that was attached to a motor shaft. The plate was prescribed an initial angular displacement and released. After being released, it would either impact a stop or continue to freely oscillate. Acceleration data and high speed video were collected during each run. Angular velocities were calculated from analysis of high speed video and the nine-accelerometer scheme. A comparison of the data during planar motion about the y-axis (no rotation about the x- and z-axes) yielded similarities in calculated angular velocity data from accelerometers and film analysis. Although peaks in angular velocity were larger in the data from film analysis, both sets of data exhibited oscillatory behavior. Similar to the current study, data was not an exact match but still provided a good estimate of the quantities of interest.

A similar investigation was conducted by Chou and Sinha in 1976. Frontal sled tests were performed at barrier equivalent impact velocities of 16, 32, and 48kph. A Hybrid II subject that was restrained by lap, shoulder and chest belts in a manner such that an upright posture was maintained during the entire sled run. Acceleration data was collected by a triaxial accelerometer located at the CG of the head and a 3-2-2-2 array of accelerometers mounted to the top of the head. In addition, high-speed video of each test was recorded. It was found that angular accelerations calculated from the 3-2-2-2 array produced larger angular velocity and angular acceleration values than those from video analysis. However, like the current study, both sets of data were found to be in agreement qualitatively.

A study by Shea and Viano (1994) investigated the accuracy of using only accelerometer data to calculate the angular rotation and x- and z- displacements of a HIII head. Angular

acceleration of the head was calculated using linear acceleration and then used to find angular rotation. Head displacements were calculated using methods similar to the current study. The HIII head and neck assembly were mounted to a platform on a mini-sled, accelerated to approximately 8m/s, and then stopped by a shock absorber at the end of the sled track. The angular rotation and head trajectory obtained from the acceleration data were compared to data from high-speed video analysis. The time histories of angular rotation, x-displacement, and z-displacement were similar but began to deviate towards the end of the test (200ms). Peak values differed by 1.8%, 0.9%, and 0.9% for x-displacement, z-displacement, and angular rotation, respectively. After analyzing the results from the mini-sled tests, two full-scale sled tests were performed. In the first test, the dummy was placed in a production seat and restrained by a lap and shoulder belt. No other vehicle components were included on the sled. The peak acceleration for this test was approximately 50g. In the second test, the dummy was placed in the production seat and restrained by a lap and shoulder belt. In addition to the seat, a High Penetration Resistant windshield was included on the test buck. For this test, the peak acceleration was 150g. Sled velocities were not specified for the two full-scale sled tests. While analytical data was similar to the high-speed video analysis, angular rotation and head displacements had larger deviations than those from the mini-sled tests. In addition, the time histories of head displacements began to deviate at approximately 100ms. The time history of angular rotation began to deviate at 60ms. The largest differences between motion data and sensor data were seen in the z-displacement of the head. Results from the full scale sled tests analyzed by Shea and Viano (1994) were similar to the results from the current study.

Limitations

There are limitations in the current study that should be addressed. Limited information was available regarding the UVA tests since these were conducted by other researchers. For example, the procedure for locating the CG of the head was not specified in the report by Bolton et al. (2006). In addition, data processing before submission to the NHTSA database was not thoroughly described in the test document.

The accuracy of the motion capture data must also be considered. The accuracy of the video motion analysis performed by UVA was not specified in the test report. However, this type of analysis is standard practice in the automotive community (Bolton et al. 2006, Padgaonkar et al. 1975, Chou and Sinha 1976, Shea and Viano 1994). The accuracy of the Vicon motion analysis system used by Beeman et al. (2011) was determined by in-house testing with a pendulum. Motion data was collected with the pendulum stationary and swinging at various amplitudes. The distances between sets of two retroreflective markers on the pendulum were determined using the Vicon motion analysis system and compared to the measured distance. The error of the system was determined to be 0.1mm to 0.2mm when the same set of cameras was tracking the markers. However the error increased slightly (±1mm) when the cameras tracking the markers switched, usually due to loss of line-of-sight of the marker. The manufacturers of the Vicon motion analysis system also performed tests to determine the accuracy of the system (Vicon Motion Systems 2008). The tests involved using specified calibration procedures to ensure that the error of the system was within 1mm.

Another limitation of this study is that it is limited to peak forward excursion (x-direction) of the head. The methods of this study, however, could be extended to analyzing entire head trajectories, given the data to do so is available. Further, this methodology can be

applied to investigate kinematics of other regions of the body. The information obtained from such studies could be used to improve or develop new computational models which explore occupant kinematics in vehicle crashes. These models can help researchers to assess injury risk and could be used in conjunction with other models of specific injuries, such as head injury (Turquier et al. 1996, Zhang et al. 2001), pulmonary contusions (Gayzik et al. 2009, Stitzel et al. 2005), rib fractures (Stitzel et al 2004), and carotid artery injuries (Gayzik et al. 2006).

Conclusions

This study compared head trajectories from motion capture data and processed accelerometer and angular rate sensor data to assess the accuracy of calculated head trajectories using sensor data. Head trajectories from motion capture data and processed sensor data were plotted up to maximum forward excursion for eight frontal sled tests. Although, trajectories calculated from sensor data did not exactly match trajectories from motion capture data, they were found to be reasonable estimates of head motion. It was found that sensor data overestimated maximum forward excursion in all but two tests. The percent difference between maximum forward excursion values from sensor and motion capture data of all eight tests was 12.01% (± 10.30%). In conclusion, data collection via accelerometers produces similar results to data collection from motion analysis. However, caution should be exercised during interpretation of the accelerometer data.

References

Beeman SM, Duma SM, Kemper AR, Madigan ML. 2011. Quantifying the Kinematics of Injury Biomechanics: Several Applications Incorporating Human Volunteers and Surrogates. *Master's Thesis*.

Bolton JR, Kent RW, Crandall JR. 2006. Passenger air bag impact and injury response using a Hybrid III test dummy and human surrogates. Charlottesville VA: NHTSA. b08380R001.

Bussone WR, Duma, SM, Gabler HC, Stitzel J, Madigan M. 2005. Linear and Angular Head Accelerations in Daily Life. *Master's Thesis.*

Chou CC and Sinha SC. 1976. On the Kinematics of the Head Using Linear Acceleration Measurements. *Journal of Biomechanics*. 9:607-613.

Cormier JM, Duma SM. 2009. Epidemiology of Facial Fractures in Automotive Collisions. *Annals of Advances in Automotive Medicine.* 53:169-176.

Duma SM, Crandall JR. 2000. Eye Injuries from Airbags with Seamless Module Covers. *Journal of Trauma*, 48(4):786-789.

Duma SM, Jernigan MV, Stitzel JD, Herring IP, Crowley JS, Brozoski FT, Bass CR. 2002. The Effect of Frontal Airbags on Eye Injury Patterns in Automobile Crashes. *Archives of Opthalmology*, 120:1517-1522.

Duma SM, Crandall JR, Rudd RW, Kent RW. 2003. Small female head and neck interaction with a deploying side airbag. *Accidental Analysis and Prevention.* 35(5):811-816.

Duma SM, Rath AL, Jernigan MV, Stitzel JD, Herring IP. 2005. The effects of depowered airbags on eye injuries in frontal automobile crashes. *The American Journal of Emergency Medicine*. 23:13-19.

Duma SM, Kemper AR, Porta DJ. Biomechanical Response of the Human Cervical Spine. *Biomedical Sciences Instrumentation*. 44:135-140.

Edmison J, Jones M, Lockhart T, Martin T. 2004. An E-textile Sytem for Motion Analysis. *Studies in Health Technology and Informatics*. 108:292-301.

Funk JR, Duma SM, Manoogian SJ, Rowson S. 2007. Biomechanical risk estimates fot mild traumatic brain injury. *Annal of Advances in Auomotive Medicine.* 51:343-361.

Gayzik FS, Bostrom O, Ortenwall P, Duma SM, Stitzel JD. 2006. An experimental and computational study of blunt carotid artery injury. *Annals of Advanced in Automotive Medicine*, 50:13-32.

Gayzik FS, Martin RS, Gabler HC, Hoth JJ, Duma SM, Meredith JW, Stitzel, JD. 2009. Characterization of Crash Indueced Thoracic Loading Resulting in Pulmonary Contusion. *Journal of Trauma*, 66(3):840-849.

Hakkarainen MJ, Bragge T, Liikavainio T, Arokoski J, Karjalainen PA, Tarvainen M. 2010. Method for Testing Motion Analysis Laboratory Measurement Systems. *Journal of Biomedical Engineering.* 132:114501.

Naunheim RS, Bayly PV, Standeven J, Neubauer JS, Lewis LM, Genin GM. 2003. Linear and Angular Head Accelerations During Heading of a Soccer Ball. *Medicine and Science in Sports and Exercise*. 35(8):1406-1412.

Padgaonkar AJ, Krieger KW, King AI. 1975. Measurements of Angular Acceleration of a Rigid Body Using Linear Accelerometers. *Journal of Applied Mechanics*. 42(3):552-557.

Shea RT, Viano DC. 1994. Computing Body Segment Trajectories in Hybrid III Dummy Using Linear Accelerometer Data. *Journal of Biomedical Engineering*. 116:37-43.

Stitzel JD, Baretta JT, Duma SM. 2004. Predicting Fracture due to blunt impact: a sensitivity analysis of the effects of altering failure strain of human cortical rib bone. *International Journal of Crashworthiness*, 9(6):633-642.

Turquier F, Kang HS, Trosseille X, Willinger R, Lavaste F, Tarriere C, Domont A. 1996. Validation Study of a 3D Finite Element Head Model Against Experimental Data. *Society of Automotive Engineers*. 105(6): 1912-1923.

Vicon Motion Systems. 2008. Information Invocation, Go Further with Vicon MX T-Series.

Zhang L, Yang KH, Dwarampudi R, Omori K, Li T, Chang K, Hardy WN, Khalil TB, King AI. 2001. Recent Advances in Brain Injury Research: A New Head Model Development and Validation. *Stapp Car Crash Journal.* 45:375-400.

CHAPTER 3
LITERARY CONTRIBUTIONS

The papers in Chapters 1 and 2 will be submitted to journals, as indicated in the table below.

Table 9. Literary contributions.

	Title	Journal
Chapter 1	An Investigation of Cranial Motion Through an Engineering Analysis of Skull Deformation	International Journal of Osteopathic Medicine
Chapter 2	Dummy and Human Surrogate Occupant Head Kinematics: A Comparison of Data Collection Methodologies	International Journal of Crashworthiness